

Applications of uncertainty analysis applied to the conceptual design of space systems

Myles A. Walton* and Daniel E. Hastings†
*Massachusetts Institute of Technology, Cambridge, MA*¹

Nomenclature

U_{L_surv}	= utility of low latitude survey mission
U_{L_snap}	= utility of low latitude snapshot mission
U_{h_surv}	= utility of high latitude survey mission
U_T	= total Utility
r	= return of an architecture (Total Utility/Lifecycle Cost)
w	= investment weightings for architectures considered
k	= risk aversion coefficient
Q	= covariance matrix
Q_D	= downside scaled semi-variance covariance matrix
S_D	= scaled semi-variance
σ	= standard deviation
$\sigma_{x,y}$	= covariance
ρ	= correlation
C_D	= cost of diversification
C_{non_recur}	= non-recurring cost of development

Abstract

One of the most significant challenges in conceptual design is managing the tradespace of potential architectures—choosing which design to pursue aggressively, which to keep on the table and which to leave behind. This paper presents the application of a framework for managing a tradespace of architectures not through traditional effectiveness measures like cost and performance, but instead through a quantitative analysis of the embedded uncertainty in each potential space system architecture. Cost and performance in this approach remain central themes in decision making, but

* Research Assistant, MIT Department of Aeronautics and Astronautics, Member AIAA

† Professor, MIT Department of Aeronautics and Astronautics, Fellow AIAA.

¹ 77 Massachusetts Ave, Bld 41-205, Cambridge, MA 02139

uncertainty serves as the focal lense to identify potentially powerful combinations of architectures to explore concurrently in further design phases.

Introduction

Consistent with the complexities of a space system, conceptual design is plagued with uncertainties from sources both identifiable and concealed. It is the job of those involved in conceptual design to wade through the uncertainty that defines the problem and arrive at decisions and architectures that, within the current level of available information, reflect the better alternative. It's clear that in uncertain environments, optimality is something of a myth. This of course is why design is part art in addition to part science. However, the simplistic assumptions of certainty of conditions, even at the embryonic stages of design, can yield detrimental conclusions. Often intractable problems, due in large part to uncertainty in the system and its the environment, are relegated to abstractions of the real problem that rely on the accuracy of current estimates. This paper lays the framework for a new way of looking at the process of exploring potential space system architectures through the lens of uncertainty, that has the potential to change the way people think about early conceptual design and the selection of designs to pursue.

Decision criteria such as cost, performance and schedule are the standard when it comes to decision making in space systems design. These measures, quantified using anything from back of the envelope estimation to expert opinion to intense computation and modeling, typically serve as the basis of the information provided to the decision maker. The mechanism to calculate information, like cost, schedule and performance, has been taught in a number of books on the design of space systems in addition to the industrial practice exercised at each contractor and continues to be the subject of a large body of research. In contrast, methods of accounting for uncertainty in predictions in space systems design have been far less published. No method has been presented, as of yet, that aggregates the types and sources of uncertainty that are typical of a space system and demonstrates an approach

to manage such information. This paper presents such an approach and goes further to develop a framework in which to explore the implications of uncertainty in different architectures.

Figure 1 presents a conceptual design flow with the inclusion of the proposed uncertainty analysis framework. Lying between concept generation and concept selection, the uncertainty analysis approach would provide useful information to the decision maker in preparation for selecting architectures to pursue. Coinciding with the vision for uncertainty to be a central decision criterion in the conceptual design of space systems, so too must the uncertainty analysis be a central component of the conceptual design process. The uncertainty analysis location, as described, would be early enough in conceptual design to positively influence decisions, while at the same time its location would be late enough, so that the problem boundaries are drawn and sources of uncertainty can be identified, assessed and quantified. Information about externalities is collected in the needs analysis and concept generation of space systems. Under the uncertainty analysis approach, further information on external sources of uncertainty would also be tapped.

This paper presents the practical implementation of the uncertainty analysis approach. For a description of the theory of the approach, see Ref. 1¹. There are three cases investigated, a space based radar space system, a space based broadband communications systems, and a space based ionospheric mapping mission. These three cases represent the three overarching segments of space systems, namely military, commercial and civil (science) missions, as shown in Figure 2. Further, the technology and conceptual architecture in each of the architectures differs significantly. These differences provide complementary implementation scenarios for the uncertainty analysis approach that provide the reader with a broader vision of how the approach could work in practice.

The first section in each case describes the overall mission as well as the conceptual design model description. All cases were modeled using the generalized information network analysis (GINA) method, as described by Shaw². The next section focuses on quantifying the architectural uncertainty

embedded in each architecture, while the third section describes the application of portfolio theory to the individual case. Finally each case is closed with insights and conclusions that each provided about the specific mission as well as the uncertainty analysis approach. The primary purpose of each case is not to describe the individual mission and modeling approach of each in depth. For this information, references have been provided. Instead, it is to demonstrate the applicability of the uncertainty analysis approach to the broad class of problems that each case represents.

TechSat 21 Mission and Model Description

TechSat 21, short for Technology Satellite of the 21st Century, is a program aimed at pushing the boundaries on the current approach to satellite systems development. Its novelty lies in concepts at both the architectural, system, subsystem and component level. The most obvious feature of the TechSat 21 architecture is the departure from the traditional monolithic satellite designs of the Milstar and Defense Support Program satellites. Unlike those systems, TechSat 21 employs collaborate clusters of satellites in what is hoped to be a more flexible, extensible, better performing and less costly architecture. Using a cluster of formation flying satellites, a synthetic aperture can be created whose properties for a variety of missions ranging from space based radar to ground moving target indication. Of course because this is a non-traditional architecture there is significant uncertainty associated with many aspects of the concepts proposed. It therefore provides a good example of the uncertainty analysis approach applied to a highly complex, high technology, and envelope-pushing problem.

To conduct a systems analysis of the potential architectures that could be employed to accomplish the TechSat 21 mission, boundaries were established as to what concepts would be evaluated. The different architectural characteristics that were considered are presented in Table 1. In the GINA terminology, these characteristics are called the design vector and a combination of the six design variables constitutes a separate architecture.

GINA Model

The TechSat 21 GINA model developed in the MIT Space Systems Lab was essential to completing this case study.³ The broad architectural concept for TechSat 21 consists of a set of collaborative, formation flying spacecraft in low earth orbit that could perform multiple missions ranging from synthetic aperture radar to ground moving target indication to signal interception. The segmentation of the TechSat 21 GINA model is presented in Figure 3. The initial modules of the simulation model are the input of the Design Vector, as previously described, and the Constants Vector. The Constants Vector represents those variables that for the enumeration of the tradespace are held constant. By doing so, architectures can be equitably compared.

Once the Design Vector and the Constants Vector have been initialized, the simulation proceeds with the Constellation Module. This module produces the orbital characteristics for the space segment that make it possible to later assess the performance of the architecture. The Radar Module quantifies the various technical performance measures in a radar context. These include: probability of detection, minimum detectable velocity of a ground target, and area search rate. The Payload Sizing module uses the inputs of the Design and Constants Vector to model an appropriate payload antenna for a given architecture. Using the Payload Module output, the Satellite Bus Module designs an appropriate configuration and sizes all subsystems to satisfy the payload requirements in terms of power and mass, as well as other conditions of the Design and Constants Vector. Once the satellites and their payloads have been modeled, the launch sequence is determined by the Launch Module. The Operations Module defines the operational requirements for the system in terms of people, ground stations, etc. The final module, the Systems Module, using outputs from the previous model as inputs, generates outcome measures for each architecture, such as total lifecycle cost as well as cost per function measures.^{3,4}

Model Results

The GINA model was evaluated for thousands of potential architectures and various outcome measures were generated to provide input to decision makers on potential architectures to pursue in further design exercises. These measures included performance measures like: probability of detecting a given target, the availability of the system, minimum detection velocity, signal to noise ratio, and area search rate. Cost measures are also generated from the simulation including launch, design and development, operations and total lifecycle cost. Although all outcome measures are of interest to the decision maker, the primary performance decision criteria chosen was probability of detection, while the primary cost decision criteria is lifecycle cost. Figure 4 presents the model results for 3000 architectures in the TechSat 21 tradespace. Each point in the chart represents a single architecture whose composition is defined by a unique design vector.

Knowing the primary decision criteria as Probability of Detection and Lifecycle Cost, the Pareto optimal front can be found for the tradespace by identifying non-dominated architectures. A non-dominated architecture is one whose performance cannot be surpassed without higher costs. Figure 5 presents the Pareto optimal front, as calculated by Jilla using heuristic search methods.³ The Pareto optimal design vector values are shown in Table 2. All the architectures in the table had an altitude of 800km, 6 planes and 42 clusters of spacecraft each having 4 satellites.

The results presented above were made using deterministic assumptions and calculations, but what kind of uncertainty is associated with each architecture selection and what is an appropriate means by which uncertainty can be managed and quantitative trade-offs can be made? By applying the uncertainty analysis approach, it is shown that there is a considerable amount of uncertainty associated with each architecture, that it can be quantified and that portfolio theory provides a central framework in which the uncertainty of the tradespace can be managed.

Uncertainty Quantification

The first step in quantifying embedded architectural uncertainty is to bound the sources of uncertainty appropriately. The possible sources of uncertainty that affect the architecture outcomes must first be identified and the designer must decide which will be included in the analysis. There are two primary reasons to not include all sources of uncertainty in practice. The first is that the analysis would quickly become intractable and the second reason is that there are some sources of uncertainty whose effects would be either very difficult to model or have little impact on the architectural uncertainties. The uncertainty categorization developed is presented in Table 3. This classification helps to both encompass the various types of uncertainty and guide designers probing for potential uncertainties and also serves as a framework for dialogue.

Once the sources are identified, each source has to be assessed for inclusion in the analysis and if included, quantified. After the identification, assessment and quantification of individual sources of uncertainty, the same GINA simulation models previously developed are used to quantify embedded architectural uncertainty through uncertainty propagation. This propagation provides one means of aggregating the individual sources of uncertainty and a method to identify contributions of individual sources to the final embedded architectural uncertainty.

Sources of uncertainty

TechSat 21 represents a revolution in the development of space systems. The program is incorporating a number of unproven technologies, architectural and operational concepts. It is truly a case of pushing the envelope. That being said, it is not surprising that the TechSat 21 has a good deal of uncertainty associated with it. Table 4 presents the attributes and value ranges that were used as potential sources of uncertainty. These uncertainties were chosen from the constants vector and represent both technical uncertainty, i.e. achievable false alarm rate and model uncertainty, i.e. tram cost density for the TechSat 21 mission.

Embedded architectural uncertainty

After the individual sources of uncertainty have been identified and quantified, the next step is to develop distributions of outcomes for each of the architectures. In this case the extreme method of uncertainty propagation was used. The first step in the technique is to list the extreme possibilities as was done in Table 4. A single state-best, worst or expected- is selected and incorporate the results into the constants vector. This vector is then used for each of the architectural simulations programmed and results are captured in an outcome vector for each architectures that includes characteristics such as performance measures such as probabilities of detection, coverage and cost measures such as development, operating and total life cycle cost. Next, a new state is chosen-best, worst, expected and the simulation is repeated for each of the architectures that are being investigated and the outcome vector is saved. This process of selecting a constants vector is repeated until outcome measures have been generated for all states.

This uncertainty quantification can be done for each of the architectures in the tradespace, or as suggested here, an efficient tradespace preprocessor can be used to develop a substantially smaller set of architectures from which to conduct uncertainty analysis. Figure 6 presents the results constituting only the Pareto optimal front architectures. The spread of the worst case from the expected case is noticeably larger than that of the spread of the best case from the expected case. This shows that the uncertainty distributions for the tradespace are left skewed meaning there is more downside than upside in the architectures being considering.

Portfolio Analysis

The previous section described the quantification of embedded architectural uncertainty. Knowing the architectural uncertainty can help decision makers in a number of circumstances, such as developing a mitigation plan once an architecture has been selected. Embedded uncertainty, along with correlation measures of how architectures behave under conditions of uncertainty, can provide the decision maker with even more potential. Using the portfolio optimization of Eq. 1, the decision maker can create

accurate trade-offs and begin to manage not the uncertainty in an *individual architecture*, but instead manage the uncertainty in a *tradespace of potential architectures*. Figure 7 shows the general characteristics of the TechSat 21 value vs. uncertainty tradespace. The Pareto optimal architectures that were determined in the traditional concept exploration of utility vs. cost tradespaces have been used here as the potential members in any portfolio.

$$\begin{aligned} \max : & r^T w - \frac{k}{2} w^T Q w \\ S.T. & \sum_{i=1}^n w_i = 1 \\ S.T. & w \geq 0 \end{aligned}$$

Eq. 1

One of the first insights seen from the value/uncertainty tradespace is that the efficient frontier is not composed of all the Pareto optimal architectures. Instead, only a few contribute to the portfolios that constitute the efficient frontier. In all, only three of the original twelve Pareto optimal architectures contribute to membership along the efficient frontier. Further, the efficient frontier does not extend beyond any individual architectures in the tradespace and instead represents a linear combination of only three assets. The reason for this is the high degree of correlation the architectures being considered share, i.e. all $\rho_i \geq 0.998$.

Quantifying Decision Maker Risk Aversion

Once the efficient frontier has been calculated, the next logical next step is to determine where the optimal strategy is for a given decision maker. As discussed in the companion paper,¹ capturing decision maker risk aversion can be relatively straightforward through the use of indifference curves and iso-utility lines. By interacting directly with the customer with this graphical technique, preferences of the decision maker can be captured and incorporated into the portfolio optimization. As previously seen, the level of aversion of the decision maker can greatly affect the optimal strategy

and this is also true in this case study. There are a total of 3 architectures that constitute membership in a portfolio somewhere on the efficient frontier and there are many combinations of those possible. Rather than chose a single decision makers aversion, two decision makers who represent these extremes as well as a more moderate decision maker are presented as well as their optimal portfolio strategy that would come from the uncertainty analysis. By using three representative decision makers, the overall sensitivities of the portfolio can be observed and outcomes compared to demonstrate the adaptability of the uncertainty analysis approach to a large range of decision makers who become involved in the development of space systems. Assume that three-decision maker's maintain risk aversion coefficient, k , values of 0.5, 2 and 3.

The first decision maker looked at has a risk aversion coefficient of 3. The iso-utility lines for this decision maker have been overlaid on the efficient frontier in Figure 8. The optimum portfolio for this decision maker resides in the lower left corner of the efficient frontier and consists of only a single architecture. Notice that the optimal strategy portfolio resides at the tangent point of the efficient frontier and the maximum utility iso-utility line. The composition of this portfolio is shown in Table 5 and consists of only a single architecture Although portfolios can suggest sets of assets to pursue, it can also suggest single assets, as in this case.

A second decision maker that was considered was one that had a moderate risk aversion, $k=2$. This decision maker's optimum portfolio strategy resides in the middle of the efficient frontier and consists of only a single asset. The relatively low risk aversion decision maker has an optimal portfolio strategy in the upper right corner of the efficient frontier again consisting of only a single architecture. The composition of the low risk aversion decision maker is shown in Table 5 and again is a single asset.

Implications of incorporating the extensions to portfolio theory

Differentiating risk from uncertainty

Presented above was the implementation of portfolio theory using uncertainty as a surrogate for risk. Here, the impact of separating the upside and downside of uncertainty is explored within a

reapplication of portfolio optimization to discover any new insights. The first step is to differentiate the risk from the uncertainty in the distribution. The risk can be found by focusing on the downside semi-variance. To do so, first adjust the variance of individual observations around the expectation as shown in Eq. 2. Then, calculate the variance of these new observation errors, as shown in Eq. 3.

$$(r_i - E(r))^- = \begin{cases} (r_i - E(r)) & \text{if } r_i \leq 0 \\ 0 & \text{if } r_i > 0 \end{cases}$$

Eq

$$S_{Downside} = 2 * E[\sum (r - E(r))^2]$$

Eq

Thus creating a downside covariance matrix as shown in Eq. 4.

$$Q_{Downside} = \begin{bmatrix} S_{d1}^2 & \rho_{2,1} S_{d2} S_{d1} & \rho_{3,1} S_{d3} S_{d1} & \dots & \rho_{n,1} S_{dn} S_{d1} \\ \rho_{1,2} S_{d1} S_{d2} & S_{d2}^2 & \rho_{3,2} S_{d3} S_{d2} & \dots & \rho_{n,2} S_{dn} S_{d2} \\ \rho_{1,3} S_{d1} S_{d3} & \rho_{2,3} S_{d2} S_{d3} & S_{d3}^2 & \dots & \rho_{n,3} S_{dn} S_{d3} \\ \dots & \dots & \dots & \dots & \dots \\ \rho_{1,n} S_{d1} S_{dn} & \rho_{2,n} S_{d2} S_{dn} & \rho_{3,n} S_{d3} S_{dn} & \dots & S_{dn}^2 \end{bmatrix}$$

Eq

Finally the portfolio algorithm is implemented in the similar manner to traditional portfolio theory, only substituting $Q_{downside}$ for Q , as shown in Eq. 5.

$$\begin{aligned} \max : & r^T w - \frac{k}{2} w^T Q_{Downside} w \\ \text{s.t. :} & \sum_{i=1}^n w_i = 1 \\ \text{s.t. :} & w \geq 0 \end{aligned}$$

Eq

Using this algorithm, an efficient frontier can be calculated in the same manner performed earlier in the case. The tradespace of uncertainty and probability of detection for full variance and semi-variance is shown in Figure 9. The efficient frontier for both the full uncertainty portfolio analysis, as well as

the semi-variance analysis is shown in the figure. An insight to take away from this chart is that there is more risk in the tradespace than would be perceived if uncertainty were used as a surrogate for risk. Another observation is that the relative position of the architectures with respect to one another has not changed and instead, the result from the semi-variance analysis is a simple shift to the right.

Now that there is a different efficient frontier, it is conceivable that decision makers should choose different optimal portfolio strategies. Using the same decision makers previously used, the low, moderate and high risk aversion, the effects that this extension provides to classical portfolio analysis are described.

The first decision maker was the high risk aversion decision maker. Under the efficient frontier using semi-variance, his optimal portfolio strategy has remained the same as previously found, as shown in Table 6. This is reasonable because there are no less uncertain architectures to pursue even though there is a higher degree of risk in the tradespace. The moderate decision maker does have a shift in his portfolio, as shown in Table 6. He has shifted to the same single asset portfolio strategy as the high risk aversion decision maker. The low decision maker's optimal portfolio strategy has remained in the upper right corner of the efficient frontier. The increased uncertainty that he is now exposed to is still not enough to adjust the low risk aversion decision maker.

Observations from TechSat 21

This case provided an illustration of the uncertainty analysis approach applied to a very advanced military space system. The level of uncertainty in the tradespace was considerable and yet, the optimal portfolio strategies for three decision makers were comprised of single architectures. Of the architectures evaluated, there was simply not enough independence of architectures with respect to uncertainty for diversification possibilities to come about. In the next two cases presented, diversification does show up as an optimal strategy; however, this case points out that not all tradespaces contain complementary architectures, that when combined yield more than any single

asset, thus making the teaching point that optimal portfolio strategies sometimes consist of single architectures.

The inclusion of uncertainty analysis did illustrate the large amount of uncertainty associated with each architecture in the tradespace, thus allowing the decision maker to base decisions, not on deterministic predictions, but ones that are cautioned by some level of uncertainty. The uncertainty analysis further illustrated the ability to compare architectures in the tradespace and understand the relative sensitivities and trace those sensitivities back to sources of uncertainty. This traceability allows designers to concentrate on either modeling with more resolution or building in enough margins in their designs to accommodate the resultant possibilities.

Broadband Mission and Model Description

This case presents the systems analysis of a space based broadband architecture. This commercial venture allows the demonstration of the uncertainty analysis framework in a context that includes aspects of market uncertainty. Numerous examples of the effects of market uncertainty can be seen on the space industry, ranging from uncertainties in launch vehicle capacity to meet the evolving needs of low earth satellite delivery to market uncertainties that defined bankruptcies in the case of Iridium and GlobalStar space systems. Where the major decision criteria for a complex system is market driven, market uncertainties should always be considered

The major feature of the architectural concept consists of a satellite network complemented by ground stations. While a space system has been chosen to service this market, the details of the architecture have not been defined and instead have been left open for defining the tradespace. Six tradable parameters define the boundaries of the tradespace, as given in Table 7.

GINA Model

Figure 10 describes the simulation flow that was employed in this case study, based on work by Kashitani.⁵ The model initiates with the definition of a constants vector that contains parameters of

the designs that remain constant across all of the architectures that are being evaluated. Examples of constants in the Broadband model are scientific constants, such as the earth's radius, and conversion factors. Other constants that are included in the Broadband model are market constants such as market size and distribution, satellite sizing ratios, and launch vehicle performance.

The simulation is relatively coarse in system design detail, but serves as a good case for analysis because of the use of market models that exemplify circumstances where market uncertainty can have the driving effects on outcomes. The flow of the model begins with a relative sizing of the spacecraft based on rules of thumb and the design vector inputs. For example, from the antenna power and antenna size, the relative mass and size of the spacecraft can be determined from sizing relationships commonly used in conceptual design.⁶ After the relative size of the spacecraft is calculated, Satellite Tool Kit® is used to propagate the satellites in their individual orbits and capture ephemeris that can be used in the coverage model. The coverage model calculates a global map of acceptable coverage that is achieved from the space segment of the architecture, based on probabilities of satellites in view. The system capacity model then generates the total subscribers that the architecture being evaluated could support. This calculation is based primarily on the link budget calculation of individual spacecraft summed over the constellation. The capacity of the architecture and its coverage are then compared with a market demand model that defines the number of likely subscribers over the course of a given year. The launch module then creates a launching scheme based on the orbital characteristics, as well as mass and size characteristics of the satellite constellation. The system component costs are then calculated as well as the total system cost that is then transformed to present valuation. The final module accepts the inputs from the previous models and generates a number of outcome measures, i.e. profit, cost-per-billable hour, etc.⁵ For the remainder of this case the billable hour-per dollar spent is used as the key decision criteria.

Model Results

Figure 11 presents the subscriber hour and system cost tradespace with dots representing the 13 Pareto optimal architectures that were calculated using a heuristic search of the design tradespace.³ These are the expected outcomes for the 13 architectures on the Pareto front, but of course there is uncertainty that surrounds each expectation that will be addressed in the next section.² From this tradespace of total subscriber hours generated by the space system and the system cost, a billable hour per dollar-invested metric (subscriber hour/\$) is developed that is used later as the single measure of value for the decision maker.

Uncertainty Quantification

Once the baseline GINA model was developed, the uncertainty quantification approach was initiated. The first step in the process was to identify the potential sources of uncertainty in architectures being investigated. Once the initial sources were identified and quantified a Monte Carlo uncertainty propagation technique was used to develop the embedded uncertainty for each architecture.

Sources of uncertainty

Because the Broadband GINA model is relatively coarse, a good deal of the uncertainty being quantified arises from the rules of thumb being used in the model simulation to generate results. However, because of the commercial nature of the case, market uncertainties are also introduced.

Cost Uncertainty

The cost module for this system used cost estimating relationships to transform mass into cost for development of the spacecraft. This served as one source of cost uncertainty. For example, The historical rule of thumb for Theoretical First Unit Cost per Kilogram is \$84,000. A normal distribution centered around \$84k with a standard deviation of \$10k was used in the simulation models to capture the expectation and uncertainty associated with the cost estimating relationship.

² A total of 17 Pareto optimal architectures were initially found; however 4 of these became infeasible under the inclusion of uncertainty and were excluded from further consideration. The infeasibility was caused by launch vehicle constraints on mass that were violated for these architectures.

Market Uncertainty

The broadband system analysis affords the opportunity to introduce market uncertainty into application. Specifically this market uncertainty is arising from the estimation of three main parameters: 1.) total market size of broadband customers, 2.) percent market capture for this project, and 3.) the discount rate used in the cash flow analysis. These three sources of market uncertainty serve as representative examples of market uncertainty. Others could have been included such as uncertainty in market geographic distribution or competition scenarios. Kelic investigated a number of market uncertainties that include those listed above in her analysis of potential space based broadband delivery systems.⁷

Uncertainty in total market size is modeled using a lognormal distribution that is consistent with pervious market analysis of the broadband market potential. A lognormal distribution is used for the obvious reasons that the market has a lower bound of zero, but a more uncertain upper bound. The expected market size was calculated on an annual basis with a six year projection.

The percent market capture is another source of uncertainty. Even with a precise market, there is no way to know what competitors you'll have and what customers will prefer. Again a lognormal distribution is used here to represent an expected market capture of 7.5% and the distribution around that.

Finally, a discount rate was used in some of the calculations to generate net present values for various architecture outcomes. The discount rate uncertainty was represented by a normal distribution with mean of 30% with a standard deviation of 7.5%.

Although market uncertainties exist in the Broadband case, by no means are market uncertainties isolated to commercial ventures. Military and civil systems also suffer from market uncertainties in a number of ways, ranging from competition to demand for the system to unknown responses from adversaries.

Model Uncertainty

Because, the simulation model was relatively coarse, there were a number of design rules of thumb used to size features of the architectures, including payload power per unit mass, mass fraction of the payload with respect to dry mass, fraction of dry mass in wet mass, and density of satellite. These rules of thumb are based on historical trends and the hope is that the previous design trends will hold for the current system. Most of these rules of thumb have associated with them an expected scaling factor and a standard error.⁸ The model uncertainties that were considered in this case were the sizing relationships for payload power per unit mass, mass fraction of the payload with respect to dry mass, fraction of dry mass in wet mass, and the density of the satellite.

Embedded Architectural Uncertainty

To calculate the embedded uncertainty in each architecture, the set of individual sources of uncertainty is built into the constants vector. The first step is to sample the constants vector under conditions of uncertainty. Once the constants vector is initialized, this vector is used for each of the potential design vector combinations under consideration and results in an outcome vector for each architecture considered.

Next, a new constants vector is selected from the distribution of possible constants vectors. The simulation for each design vector combination under consideration is repeated, resulting in a second set of outcome observations for each architecture evaluated. This process of selecting a constants vector is repeated many times until a populated distribution of outcome measures can be generated. The number of runs is only limited by the computation required and time allowed, as many simulation models for every design vector combination can take 5-10minutes.

The end result of the uncertainty propagation is an ordered set of outcomes for every architecture considered. This data can be used to create statistical measures of uncertainty for a single architecture and also the pair-wise correlation coefficients that are necessary in portfolio optimization. Figure 12 presents a snapshot of the embedded uncertainty that was calculated for each architecture on the

Pareto optimal front. The diamonds represent the expected value of the architecture in terms of system cost and total subscriber hours, while the ellipses represent the uncertainty of each architecture in both dimensions.

Portfolio Assessment

Once the embedded architectural uncertainties have been calculated, the portfolio assessment can be applied. The portfolio assessment provides a context in which trade-offs of uncertainty and value, subscriber hour/\$, can be made. Using an expected return and covariance matrix based on 100 observations of 13 architectures, the portfolio optimization algorithm was applied to generate the efficient frontier.

Using an architecture portfolio analysis flight simulator, the designer and decision maker can dynamically explore trade-offs between uncertainty and function-per-cost. Figure 13 provides a screen shot of the flight simulator. The dot indicates the current portfolio, while the weight of each architecture in the portfolio is listed on the right hand side along with the expectation of function-per-cost and uncertainty. An immediate observation from the portfolio tradespace is the clear demarcation of GEO, MEO and LEO architectures along measures of value and uncertainty.

Quantifying Decision Maker Risk Aversion

Once the efficient frontier has been calculated, the next logical next step is to determine the optimal strategy for a given decision maker. Rather than chose a single decision makers aversion, two decision makers who represent these extremes are presented as well as a more moderate decision maker and their optimal portfolio strategy that would Assume risk aversion coefficients, k , calculated for three decision makers are 0.03, 0.1, and 1.

Decision maker with high risk aversion optimal portfolio strategy

The first decision maker looked at was the highly risk averse decision maker with a k value of 1. A highly risk averse decision maker would expect to find themselves in the lower left hand corner of the efficient frontier and that is exactly what is shown in Figure 14. The optimal investment strategy

where the highest iso-utility curve becomes tangent to the frontier is shown in the figure. The composition of the optimal strategy is defined in Table 8. There were lower risk assets for which the decision maker could have invested, such as the one GEO architecture on the Pareto optimal front, but this decision maker desired more return than the lower risk architectures could provide.

Decision maker with moderate risk aversion optimal portfolio strategy

The second decision maker investigated has a k value equal to 0.1. In most cases this value would not be considered a “moderate” level of risk aversion, but the phrase is used here to show the relative preference to uncertainty of three decision makers. The composition of this portfolio lies at a single architecture, a LEO architecture consisting of 40 satellite constellation each with a 2 m² antenna and 1 kW power.

Decision maker with low risk aversion optimal portfolio strategy

The third decision maker has a very low level of risk aversion, $k=0.03$. The optimal strategy for this decision maker, as one might expect, it resides in the upper right corner of the efficient frontier. The composition of the portfolio is described in detail in Table 8. The reason for large LEO architectures dominating this portfolio is that the larger the constellation of satellites and the more capacity a system has to achieve subscriber hours if the market conditions are good. However, under adverse market conditions, the system won't achieve the subscribers expected and it will have required a significant capital investment to construct it. Notice that one of the assets suggested is only 2% of the portfolio. In practice 2% of an architectural investment would most likely not be enough to produce tangible benefits, so this percentage might best be distributed amongst the other two assets.

Implications of incorporating the extensions to portfolio theory

The classical implementation of portfolio theory has been presented using uncertainty as a surrogate for risk, but in fact, the two can be separated, as shown below through the use of semi-variance. Further, the low risk aversion decision maker has a suggested optimal portfolio that consists of more

than one asset. What is the extra cost of that portfolio and how should a cost benefit trade be made? To find the answer, the correlation coefficient of the portfolio members is used as a starting point.

Differentiating risk from uncertainty

Using the algorithm in Eq. 5, an efficient frontier can be calculated in the same manner performed earlier in the case. The efficient frontier for both the full uncertainty portfolio analysis, as well as the semi-variance analysis is shown in Figure 15. There is less risk in the tradespace than would be perceived if uncertainty were used as a surrogate for risk.

Using the same decision makers previously used, the low, moderate and high risk aversion, the effects that this extension to classical portfolio analysis would provide are discussed. The first decision maker was the high risk aversion decision maker. Under the efficient frontier using semi-variance, his optimal portfolio strategy has remained the same as was previously found in Table 9.

The moderate risk aversion decision maker has seen no shift in his optimal portfolio strategy. Although there is less perceived risk in the tradespace under the semi-variance calculation, the same architecture is still retained. However, the low risk averse decision maker has seen a shift in strategy. He previously had a portfolio of three assets as an optimal portfolio strategy, but now has two, namely the architectures that had the highest values.

Cost of diversification

Some of the optimal portfolio strategies that have been found in this case have included more than one asset and therefore more than one architecture to pursue in design. In order to calculate the exact cost to diversify into a portfolio, the individual assets should be closely looked at by the designers and decision makers. For example, two LEO architectures with 45° inclination operating at 1kW and 2m² antennas and having only a small difference in the number of satellites in slightly different planes will probably not incur twice the design cost of a single architecture because of the commonality between the two architectures. In contrast, a two asset portfolio with a very large LEO architecture requiring

many ground stations and a two satellite GEO architecture might represent a significantly higher cost to develop than either of the two individually.

A relative measure of the cost of diversification is used to judge the relative extra cost of carrying a portfolio based on the correlation of assets in the portfolio, as described in the companion paper¹. For an example, the low risk aversion decision maker under the full uncertainty distribution would have a cost to diversify equal to 0.5% of the cost to design the architecture with the design vector {LEO, 45, 5, 8, 1, 2} plus 0.1% of the cost to design the architecture with the design vector {LEO, 45, 7, 10, 1, 3}. Therefore the total cost to proceed with the portfolio would be the cost of designing the majority constituent in the three-architecture portfolio plus this additional cost to diversify. This type of calculation can provide the basis for additional consideration by the decision maker on whether or not to proceed with the portfolio strategy. Again the cost to diversify calculated here is a figure of merit and represents a relative estimate on what the cost could be. The actual cost to diversify will be case specific and should be looked at carefully by the designers and decision makers.

Observations from Broadband case study

This case demonstrated the applicability of the uncertainty analysis approach to space based broadband communications architecture. Market and model uncertainty were explored as primary sources of uncertainty and the case demonstrated how significant these sources could be to the overall value of a given architecture, with some architectures maintaining 50% uncertainty. The role of downside semi-variance focus was also demonstrated, in contrast to a full uncertainty, and the impact that such separation would have on the decision maker's optimal strategy with the same level of risk aversion was shown.

The intuitive observations that comes from the analysis such as LEO architectures having predominantly greater uncertainty than MEO and GEO architectures is reinforcing to current speculations, but the case provides a quantitative base for exploring the intuition in more detail.

Moreover, an interesting final note on this case is how real world systems are acting with respect to the efficient frontier that was developed. The Teledesic Space System has been in development for some time. Initially conceived as a very large, LEO constellation of satellites, the system would provide global broadband capability with very low latency and at a reasonable price. The original concept was released in 1994 as having 840 satellites at development cost of \$6.3B and total life cycle cost of \$17.8B.

In 1998, Teledesic went through a dramatic redesign from 840 satellites in LEO to 288 satellites. As was shown in the analysis, this shift to fewer spacecraft lowered the potential market capture of the system, but also lowered the exposure to risk that the system would have from the upfront development cost investment.

In February 2002, a Teledesic architecture redesign was publicly released consisting of 12 satellites in MEO at a development cost of \$1B and 18 more MEO satellites deployed at a later date to supplement coverage to achieve global capacity. Again, this is a downward movement on the efficient frontier, opting for less capacity and subscriber hours/\$, but at a significantly lower cost than the LEO systems.

Terrestrial Observer Swarm Mission and Model Description

The ATOS Mission (short for the first iteration, A, in a series of Terrestrial Observing Swarms missions) has the primary objective of collecting and disseminating fine measurements of the ionosphere. This data would be used by the science customer as inputs to a simulation model used for describing the behavior for the ionosphere. An understanding of the ionosphere's composition at fine detail would allow for more accurate prediction and mitigation of errors in communication and location measurement. Potential tactical benefits of a detailed mapping of the ionosphere begin to paint a clear picture of the potential value of such a mission beyond the pure science of ionospheric mapping.

The ATOS Mission

Given the significant impact of the ionosphere and its variability on communications and navigation, the science- and even broader space-community are interested in the accurate modeling and prediction of ionospheric dynamics. The overarching goal of the ATOS mission was to design a space system that captured both the large scale and time-scale aspects of the ionosphere, as well as the detailed, small time-scale fluctuations that are so unpredictable. More detailed time resolved measurements of the ionosphere are essential to predictive modeling of RF scintillation. One of the most interesting features of the ATOS model developed was the use of utility measures to define “goodness” in the tradespace of architectures. Instead of using a set of performance measures, such as usable bytes delivered or resolution and accuracy, a non-traditional approach, utility theory⁹, was applied to the problem of balancing the many sets of customer preferences that were involved in the program.

Utility theory allows the designer to capture preferences of the customer in mathematical equations that provide for customer-in-the-loop trade-offs, while not necessarily requiring their physical presence. Of course, the physical collocation of the customer can be clarifying and perhaps more accurate and adaptive to unforeseen circumstances than utility theory, but can take a toll on the customer in terms of time invested in the project.

Five concepts to accomplishing the ATOS mission were investigated, as shown in Figure 16. The ionosphere is represented by the dotted patterns in each of the five charts, while the boxes represent the notional satellites that are part of the overall space system. The in-situ approach was the one employed in the ATOS architecture. Perhaps the easiest to conceive of all the possible measurement schemes, the concept would rely on direct measurement of ionospheric conditions as the individual satellites passed through it. The payload would be a passive payload consisting primarily of Planar Langmuir Probes (PLPs) to record charged particles densities. This approach has the benefits of

having a relatively simple passive payload that requires little power, mass and records data that needs little post-processing to arrive at useful information for the customer.

Derived Utility Function

The utility of the ATOS system was derived from an architecture's ability to satisfy three distinct sub-missions desired by the customer. The first, the low latitude survey mission, was an equatorial region survey that would identify unstable regions of the ionosphere near the equator. The second mission, the low latitude snapshot mission, would require the space system to initiate an extensive data collection of an unstable region once the first mission identified a instability. The third mission was to perform a high latitude survey that would accurately measure relative ionospheric density correlated with GPS-to-ground data.

The low latitude survey mission was to measures the low latitude characteristics of the ionosphere at a sampling rate of approximately 1Hz, as shown in Figure 17. From this information, the customer's model could be populated with the large-scale characteristics of the ionosphere.

The low latitude snapshot sub-mission would be important once the survey mission identified a ionosphere disturbance. Using a swarm of satellites, fine-scale measurements of the anomaly would be collected. As shown in Figure 18, satellites at different separation distances are useful to the customer, because at large separation distances the overall shape and characteristics of the disturbance would be captured, while small separation distances would provide more baseline measurements of variability within the disturbance. All this data would feed into the customer's model and provide better predictability for future communications outage planning.

The last sub-mission is a high latitude survey. The major charged particle concentration in the ionosphere is centered about the equatorial band and the high latitude region. Although not as significant a sub-mission as the low latitude missions, the high latitude mission would provide further population of the science communities global ionospheric model and prediction ability. Typically, the

high latitude region is less turbulent than the low latitude region and therefore, the science community is only interested in the survey mission as opposed to the survey and snapshot mission. Figure 19 represents the notional space segment that could accommodate the high latitude mission. The desirable separation among satellites in this mission is about 75km in the direction of longitude and latitude and 20km in the direction of altitude. In the low latitude region, the ionosphere is fairly constant with altitude, this assumption does not hold with the high latitude mission. Further, there would be added value to the science community if GPS occultation measurements could be taken as well to correlate the data produced by in-situ measurements of the swarm.

From the above missions, utility functions were calculated for each of the missions, as a function of each mission's attributes, as notionally shown in Eq. 6, Eq. 7, and Eq. 8. For example, the low latitude survey mission was a function of individual sample observations and the location and time of day of each measurement.

$$U(Low_Surv) = f(X_1, X_2, \dots, X_m)$$

Eq

$$U(Low_Snap) = g(Y_1, Y_2, \dots, Y_m)$$

Eq

$$U(High_Surv) = h(Z_1, Z_2, \dots, Z_n)$$

Eq

Additionally, a total architecture utility variable was defined as a weighted sum of the two separate mission utilities, as shown in Eq. 9. Although this is a simple linear aggregation of the multiple elements of utility it provided a first look at how ideas of utility could be incorporated into the space systems conceptual design process. Considerable progress has been made on subsequent design iterations that exploit the full potential of multi-attribute utility theory.

$$U(Total) = U(High_Surv) / U_{\max}(High_Surv) + 2 * (U(Low_Surv) + U(Low_Snap)) / (U(Low_Surv) + U(Low_Snap))_{\max}$$

Eq

The design vector that was developed to define the tradespace of architectures that would be investigated is presented in Table 10 and graphically in Figure 20. The design vector consisted mainly of orbital parameters, as the mission was driven by the in-situ locations of individual satellites throughout the mission lifetime.

System Analysis Model

The conceptual design simulation models developed during the ATOS design effort were based on heritage models developed under the generalized information network analysis (GINA) method¹⁰, but actually went beyond the original approach by applying utility theory to capture the preferences of the customer in the simulation. A utility function was formulated, as described earlier, and incorporated into the system simulation, as presented in Figure 21 to generate outcome measures that would enable informed trade-offs of potential architectures.

Model Results

Over four thousand architectures were evaluated using the simulation model. After calculating the expected outcomes for these thousands of potential architectures, the tradespace was explored along the fundamental utility and cost measures developed in the early problem formulation. Figure 22 shows how the tradespace took shape in terms of low latitude utility, high latitude utility and cost. Each shaded square in the chart represents at least one specific architecture concept, as defined by a unique design vector. In the figure, the two dimensions of customer utility have been plotted and the shaded squares represent the life-cycle cost of a given architecture. The first intuitive conclusion that can be drawn from this tradespace is that utility increases with increasing cost. It is further evident though that there are some relatively inexpensive architectures that accomplish the low latitude mission quite well, but don't perform very well in the high latitude mission. These types of multi-dimensional utility plots can be used with the customer to revisit the relative importance of individual missions.

Exploring the tradespace further, the individual points can be identified by what architecture they represent, as well as what characteristics drive the performance outcomes. Figure 23 represents the total utility and cost predicted outcomes for 1380 designs, which are represented as diamonds in the plot. By using the total utility function in Eq. 9, overall architectural preferences can begin to be observed. For example the highest utility-per-dollar or the highest total utility architecture can be found, as shown in the figure. Interesting to notice is that the highest utility-per-dollar architecture is separated from a “bad” design by only a few design parameters changing.

The ATOS mission analysis produced a fairly large tradespace with varying outcome measures and there are some very good designs, but there are also some less desirable outcome designs. The horizontal bands that are formed are due to the number of satellites in the swarms, which drive the lifecycle cost of the mission. Other dimensions of the design vector drive the outcome value for total utility.

Uncertainty Quantification

Uncertainty investigation is limited to the Pareto optimal front of architectures in the tradespace, primarily for the reason of computational efficiency. The set of Pareto optimal architectures includes all non-dominated architectures. In the ATOS case, a non-dominated architecture is one who’s performance cannot be improved without paying a higher lifecycle cost. The true Pareto optimal architectures in the ATOS tradespace consist of only 6 architectures, however. Therefore to increase the pool of potential architectures to draw upon in the portfolio analysis, 24 additional near Pareto optimal architectures were chosen to use in the uncertainty analysis approach. These 30 architectures are graphed in Figure 24.

Sources of uncertainty

Technical Uncertainty

The major technical uncertainty that was included came from the mean time to failure (MTTF) for a single satellite in the constellation. Because the mean time to failure is a representative reliability of the

entire satellite, it is a very difficult number to measure. Small satellites such as those presented have previously used 500 months as the mean time to failure. However, there are not a lot of these distributed satellite systems in operation, so the reliability warranted the inclusion of uncertainty bounds. A normal distribution with a standard deviation of 50 months was used to represent the uncertainty in MTTF.

Cost Uncertainty

The cost uncertainty arose from both cost to develop and the cost of operations. The uncertainty in the cost of development of the satellite bus was captured using the standard error in the historical cost estimating relationships used in the simulation models. The development cost uncertainty for the payload was also included. The operations cost uncertainty arose from uncertainty in the estimation of the individual sources that contribute, such as the number of engineers and operators required for maintaining the system and the uncertainty in the cost of ground software and equipment.

Utility Uncertainty

Because this case relied on utility as the key decision criteria, an element of utility uncertainty was included in the analysis. The combined low latitude mission and high latitude mission were difficult for the customer to distinguish in terms of precise relative value, so a nominal value of 2:1 was used as the utility ratio of the combined low utility mission to the high utility mission as was shown in Eq. 9. Instead of using this ratio, the relative worth of the high latitude mission over the low latitude mission was modeled as a probabilistic density function with a mean of 2 and a standard deviation of 1.

Model Uncertainty

The model uncertainty in the ATOS case study arose from the designers in ability to precisely quantify different aspects of the system through mathematical formulation. Instead, design rules of thumb or parametric relationships are used that are based on historical observations. Two model uncertainties in the case of ATOS were the satellite density, which is used to calculate the derived mass and overall

structure within the model, and the learning curve used to estimate production costs for more than one satellite.

Embedded Architectural Uncertainty

Once the sources of uncertainty have been identified and each has been quantified and inserted into the constants vector, a Monte Carlo sampling routine is conducted with the goal of developing distributions of outcomes for each of the architectures evaluated. These distributions characterize the embedded architectural uncertainty and are used to compare architectures and their responses to the various sources of uncertainty.

The end result of the uncertainty propagation is an ordered set of outcomes for every architecture considered. This data can be used to create statistical measures of uncertainty for a single architecture and also the pair-wise correlation coefficients that are necessary in portfolio optimization. Figure 25 presents a snapshot of the embedded uncertainty that was calculated for each architecture on the Pareto optimal front. The points represent the expected value of the architecture in terms of cost and total utility, while the ellipses represent the uncertainty of each architecture in both dimensions.

Normality in Architectural Distributions

Portfolio theory abstracts uncertainty characteristics to simple measures of expectation and variance that are consistent with gaussian distribution. The individual architecture uncertainty distributions should be investigated to satisfy this assumption that the characteristics of the uncertainty distribution can indeed be captured by these simple measures. Normality can be tested using statistical measures such as skewness and kurtosis as well as graphical techniques. Using the Shpiro-Wilk test for normality, the hypothesis for normality could not be rejected for any of the architectural distributions created in the ATOS systems analysis.

Portfolio Selection

Using the quantified uncertainty for each architecture, and knowing the correlation of outcomes, portfolio theory can be applied with the goal of defining optimal investment strategies. Using an

expected return and covariance matrix based on 60 observations of 30 architectures, the portfolio optimization algorithm was applied to generate the efficient frontier. Figure 26 presents the efficient frontier, as derived under the classic portfolio optimization algorithm in Eq. 1. The efficient frontier extends beyond the performance achieved by any single architecture, as shown in Figure 27. This is an important finding as it shows that portfolio theory can provide more potential to the decision maker than would otherwise be possible with a single asset. The reason for the extension beyond any single architecture can be traced back to Figure 23. Notice that some architectures achieve a very high level of low latitude value at low cost but perform the high latitude mission poorly, whereas others perform well in both low and high latitude missions. Because of these two different approaches to achieving total value, there arises a chance to diversify uncertainty. The amount diversified is not enormous, but it is measurable and presents one of the first illustration that portfolio assessment in space systems can help decision makers achieve higher returns for a given level of uncertainty than they otherwise could with single assets.

Quantifying Decision Maker Risk Aversion

Rather than chose a single decision makers aversion, two decision makers are presented who represent these extremes as well as a more moderate decision maker and the optimal portfolio strategy that each would follow from the uncertainty analysis. By using three representative decision makers, the overall sensitivities of the portfolio can be observed and outcomes compared to demonstrate the adaptability of the uncertainty analysis approach to a large range of decision makers who become involved in the development of space systems.

Decision maker with high risk aversion optimal portfolio strategy

The first decision maker looked at has a risk aversion coefficient, k , equal to 2. This is a relatively high degree of risk aversion and so it is expected that this decision maker's optimal portfolio strategy reside in the lower left corner of the efficient frontier, and that is exactly what Figure 28 shows. To identify this point, the efficient frontier is plotted and then overlaid with iso-utility curves for a given decision

makers aversion level. The three convex curves represent the iso-utility curves for a decision maker, each increasing in utility as they move to the upper left. Therefore the optimal portfolio investment strategy would lie at the tangent point of the iso-utility curves and the efficient frontier, as show in Figure 28.

The composition of the optimal portfolio for this decision maker is 48% of one architecture and 52% of another, as shown in Table 11. The two architectures that have been selected behave differently enough to move the curve beyond a simple linear combination of the two and provide measurable value through diversification. A strategy has been created that has less uncertainty than either of the portfolio assets. These kinds of non-intuitive synergies can only be found through a method such as the one presented here. The majority of the portfolio is occupied by the architecture that was identified as having the maximum utility in the tradespace in Figure 23, while the remaining portfolio includes a much smaller architecture of only 2 satellites, compared to 26, and has a much smaller cost. The two combine synergistically in this portfolio because the two architectures are achieving total utility/\$ in two ways. The 26 satellites architectures is achieving both the low and high latitude missions, but at a high price. The 2 satellite mission is achieving good results on the low latitude survey sub-mission, but doesn't have enough satellites to do a good job at either the low latitude snapshot mission or the high latitude survey. On the other hand, the 2 satellite architecture is inexpensive, thus it achieves a good total utility/\$. Because the approaches of the two architectures are different with respect to total utility/\$, the effects of uncertainty on each of the architectures outcome measure have been different.

Decision maker with moderate risk aversion optimal portfolio strategy

The next decision maker presented has a more moderate risk aversion coefficient, k , of 1. This decision maker's strategy lies in lower left half of the efficient frontier, but still relatively far from the previous decision maker. Notice that a decision maker with this level of risk aversion can be

accommodated in the portfolio analysis technique. However, without the creation of portfolio, the decision maker would have to settle for single assets that meet his risk aversion criteria but achieve much lower total utility/\$, or the decision maker would need to accept a higher level of risk than their aversion coefficient would predict them to be comfortable with to achieve a high level of total cost/\$. The ability of portfolio theory to create continuous investment strategies is another benefit that can't be achieved with single assets.

The composition of the optimal portfolio is for the moderate risk averse decision maker is presented in Table 11. Once again, the majority of the portfolio is occupied by the 26 satellite architecture as was seen with the previous decision maker. The rest of the portfolio has changed though. This decision maker is looking to get more return and willing to accept more risk, so two architectures enter the portfolio that have greater returns than the architectures in the highly risk averse decision maker case, but also greater uncertainty. The higher returns in terms of Total Utility/\$ come about because the 4 satellite architectures, although achieving less overall mission utility, do so using a far less proportional cost.

Decision maker with low risk aversion optimal portfolio strategy

Finally, a decision maker who has a relatively low risk aversion coefficient, k , of 0.4 is investigated. The optimal portfolio strategy lies in the upper right corner of the efficient frontier. With a relatively low level of risk aversion, this type of decision maker is trying to get the most value out of the system with relatively little worry about the risk that the solution might carry.

The composition of the optimal portfolio is presented in Table 11. Notice one architecture from the moderate risk averse decision maker is kept, but a new architecture has been added as well. This architecture should be familiar, as it was called out in Figure 23 as the best value design. Indeed, this architecture did have the highest total utility/\$, but it also had the highest level of uncertainty for any of the architectures.

Implications of incorporating the extensions to portfolio theory

Although classic portfolio techniques were used above, the extensions to portfolio theory, as described in Ref. 1, could also be applied to glean any new information. The first extension that can be made is separating the risk from the uncertainty previously used. This separation can be useful to illustrate to decision makers that architectures are more or less risky than their uncertainty distributions might lead to one to believe. The second extension that is used is to quantify the cost of carrying a portfolio of architectures, rather than any single asset.

Differentiating risk from uncertainty

Using this algorithm in Eq. 5, the semi-variance scaled efficient frontier with the full uncertainty distribution efficient frontier is shown in Figure 29. The efficient frontier for both the full uncertainty portfolio analysis, as well as the semi-variance analysis is shown in the figure. An important insight to take away from this chart is that by using the full distribution variance, rather than the downside semi-variance, the risk to a given decision maker was overestimated.

The first decision maker was the high risk aversion decision maker. Under the efficient frontier using semi-variance, his optimal portfolio strategy has changed only in percentage investment in each of the assets in his portfolio, as shown in Table 12. The optimal portfolio now has a higher degree of emphasis on the higher return asset. The moderate decision maker has kept two of the previous three asset portfolio. Again, there is an overall percentage investment increase in the higher return asset.

The low risk aversion decision maker has moved his optimal strategy to a one-asset portfolio.

Although there did not appear to be a large degree of shift in the efficient frontier using semi-variance in place of full uncertainty, there was enough to move 17% investment of another architecture out of this portfolio, so that 100% of the resources could be devoted to the highest value system.

Cost of diversification

Some of the optimal portfolio strategies suggested in this case have included more than one asset and therefore more than one architecture to pursue in design. In order to calculate the exact cost to

diversify using a portfolio, the individual assets should be investigated by the designers and decision makers. For example, two 4 satellite architectures with similar characteristics differing only in altitude by 200km will probably not incur twice the design cost of a single architecture because many of the similarities in each architecture can be design for both. In contrast, a two-asset portfolio with a 26 satellite architecture at very large separation distance and a two satellite swarm at very small separation distance architecture might represent a significantly higher cost to develop than either of the two individually.

A measure of the cost of diversification can be used to judge the relative extra cost of carrying a portfolio based on the correlation of assets in the portfolio, as presented in Ref. 1. For example, the high risk aversion decision maker under the full uncertainty distribution would have a cost to diversify equal to 33% of the cost to design the 2 satellite architecture. This high cost to diversify is based on the low correlation that exists between the two assets, 0.598. In contrast the cost to diversify of the low risk averse decision maker would be only 3.5% of the cost to design the 4 satellite architecture in the portfolio. This lower additional cost is due to the higher degree of correlation that exists, 0.965.

Observations from ATOS case study

A proposed uncertainty analysis approach has been presented and implemented on a representative scientific space mission. This case provided an opportunity to implement the uncertainty analysis approach in the context of a scientific space system analysis. The ATOS case study demonstrated the use of the uncertainty analysis method in a system exploration that centered around utility/\$ as a fundamental decision criteria.

This approach captures the benefits that portfolio analysis can provide to a decision maker by creating investment strategies for design that achieve higher value for lower uncertainty than would be possible with any single asset. Illustrated by the high risk averse decision maker whose optimal portfolio consisted of architectures that achieved value through different approaches and therefore reacted

differently to uncertainty. Finally the focus on downside of uncertainty was shown to have impact on the optimal investment strategy of different decision makers.

Conclusions

The application of an uncertainty analysis approach has been presented in the context of three mission classes of space systems. The broad applicability of the uncertainty analysis framework has been demonstrated in the design process where structured modeling and simulation is done that enables the production of performance outcome distributions for outcomes. Further, it has been shown in some cases that portfolios of solutions lead to higher expected value than any single asset can attain.

Acknowledgements

The authors would like to thank Professors Ed Crawley and Earll Murman, and Dr. Joyce Warmkessel, Dr. Hugh McManus, Dr. Cyrus Jilla, and Dr. Annalisa Weigel (all of MIT) for their insights and feedback on this research work. Dr. William Borer, Dr. Willam Kaliardos, Dave Ferris, Andre Girard, Adam Ross, Dan Thunnisen and Brandon Wood produced much of the ATOS simulation models. The authors gratefully acknowledges the financial support for this research from the Space Systems Policy and Architecture Research Consortium (SSPARC), a joint research program funded by the U.S. government involving the Massachusetts Institute of Technology, the California Institute of Technology, and Stanford University.

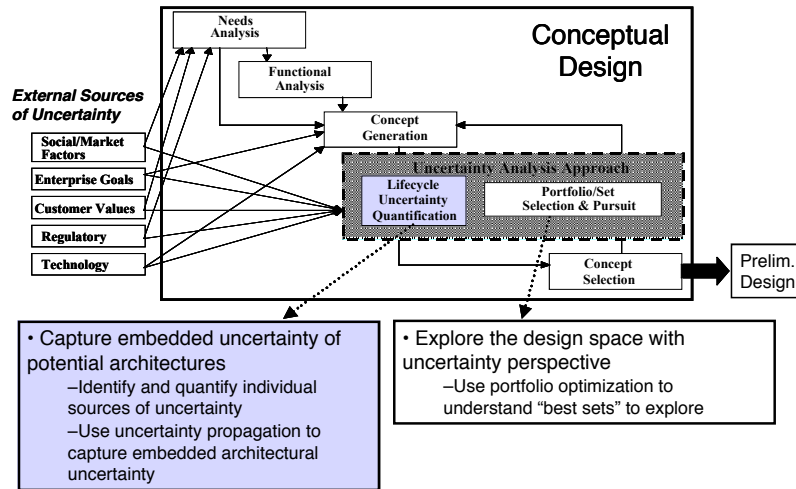


Figure 1: Insertion of the uncertainty analysis approach in conceptual design

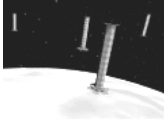
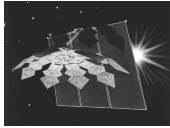
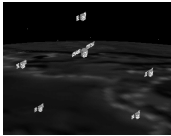
	<p>Mission Name: TechSat 21 (Military)</p> <p>Value Measure: Probability of Detection/\$</p> <p>Uncertainty Measure: StdDev(Pd/\$)</p>
<p>Mission Name: Broadband System (Commercial)</p> <p>Value Measure: Billable Hour/\$</p> <p>Uncertainty Measure: StdDev(BH/\$)</p>	
	<p>Mission Name: ATOS (Science)</p> <p>Value Measure: Total Utility/\$</p> <p>Uncertainty Measure: StdDev(TU/\$)</p>

Figure 2: Three case studies summary

Table 1: Design vector for the TechSat21 Satellite System

Name	Description	Potential Values
Altitude	The operating altitude of the TechSat21 constellation	500-1500km
Number of Satellites	The number of satellites in each cluster/swarm	4-16
Number of Cluster	The number of cluster/swarms that comprise the constellation	2-100
Number of Planes	The number of orbital planes occupied by the constellation	2-10
Antenna Power	Antenna Transmission Power	100-1kW
Antenna Diameter	Antenna Aperture Diameter	0.5-3m

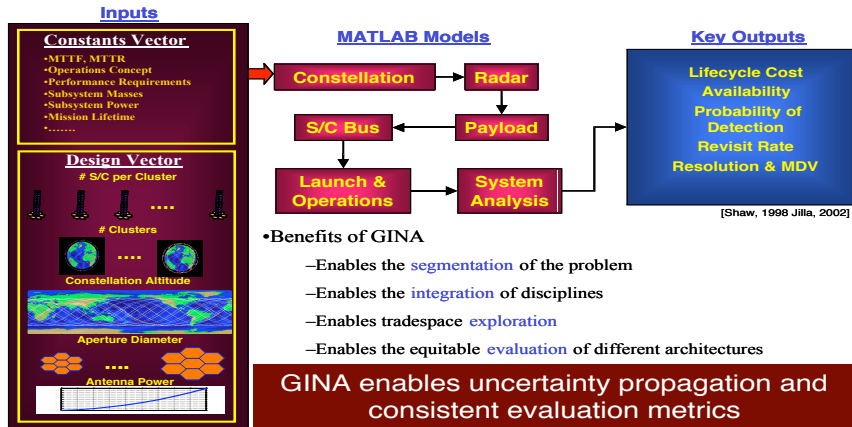


Figure 3: GINA Model Flow Chart

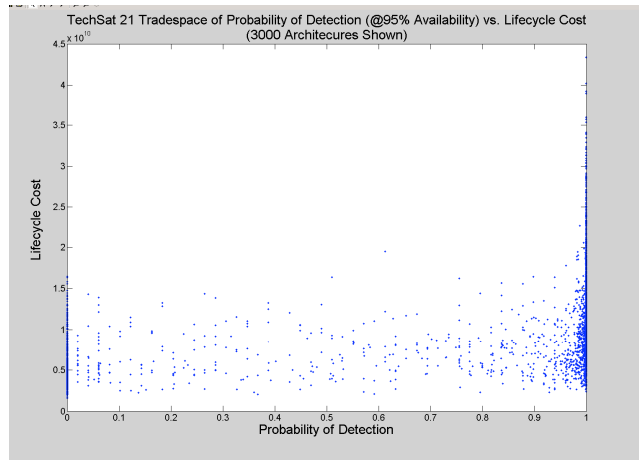


Figure 4: TechSat 21 Tradespace

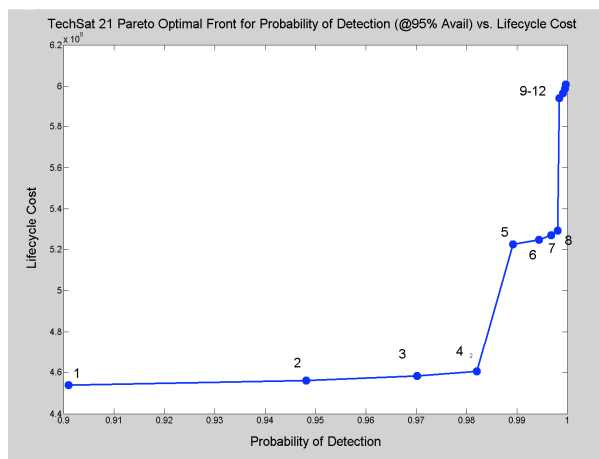


Figure 5: Pareto Optimal Front for TechSat 21 Architectures

Table 2: TechSat 21 Pareto Optimal Architectures and Outcome Measures

Architecture	1	2	3	4	5	6	7	8	9-12
Ant Diam	2.5	2.5	2.5	2.5	3.0	3.0	3.0	3.0	3.5
Ant Pow	700	800	900	1000	700	800	900	1000	700-1000
P(d)	90.0%	95.0%	97.0%	98.2%	98.9%	99.4%	99.7%	99.8%	99.8%-99.9%
Lifecycle Cost (\$B)	4.57	4.59	4.61	4.64	5.18	5.20	5.22	5.24	6.00-6.07

Table 3: Uncertainty Categorization

Development Uncertainty	Operational Uncertainty
Political Uncertainty- uncertainty of development funding instability	Political Uncertainty- uncertainty of operational funding instability
Requirements Uncertainty- uncertainty of requirements stability	Lifetime Uncertainty - uncertainty of performing to requirements in a given lifetime
Development Cost Uncertainty- uncertainty of developing within a given budget	Obsolescence Uncertainty – uncertainty of performing to evolving expectation in a given lifetime
Development Schedule Uncertainty- uncertainty of developing within a given schedule profile	Integration Uncertainty – uncertainty of operating within other necessary systems
Development Technology Uncertainty- uncertainty of technology to provide performance benefits	Operations Cost Uncertainty – uncertainty of meeting operations cost targets
	Market Uncertainty-uncertainty in meeting demands of an unknown market
Model Uncertainty	

Table 4: TechSat 21 Modeled Sources of Uncertainty¹

Attribute	Best Value	Expected Value	Worst Value
Mission Lifetime	9 years	10 years	11 years
Radar Freq.	10.2E9 Hz	10E9 Hz	9.8E9 Hz
Ant Trans. Duty Cyc.	0.045	0.05	0.055
Radar Cross Section	10.2 m ²	10 m ²	9.8 m ²
Required Range Res.	240m	250m	260m
Tram Mass Dens.	8 kg/m ²	6 kg/m ²	4 kg/m ²
Tram Elec. Dens.	7 kg/m ²	5 kg/m ²	3 kg/m ²
Tram Cost Dens	1.25E6 \$/m ²	1E6 \$/m ²	0.75E6 \$/m ²
Tram Elec. Cost Dens.	1.25E6 \$/m ²	1E6 \$/m ²	0.75E6 \$/m ²
Stowed Depth	0.6 m	0.5 m	0.4 m
# PrimexPPT	6	4	3
Mass Primex PPT	2 kg	1.5 kg	1 kg
Pow. Primex PPT	20 W	1 W	1 W
#Micro PPT	12	10	8
Mass Micro PPT	0.5 kg	0.2 kg	0.2 kg
Pow Micro PPT	10 W	0.5 W	0.4 W
Star Sens. Mass	2.5 kg	0.7 kg	0.5 kg
Star Sens. Pow	20 W	4 W	4 W
Magnometer Mass	1.2 kg	0.13 kg	0.13 kg
Mangonmeter Pow	1 W	0.5 W	0.5 W
# Torque Rods	4	3	2
Mass Torque Rods	0.6 kg	0.45 kg	0.4 kg
Power Torque Rods	2 W	1.3 W	1 W
MB per Chip	48 MB	64 MB	96 MB
Mass per Chip	1 kg	0.5 kg	0.5 kg
Bat. Power Density	45 W hr/kg	51 W hr/kg	60 W hr/kg
Operators per Satellite	1.2	1.1	1
MTTF	450 months	498 months	550 months
MTTR	2 months	3 months	4 months

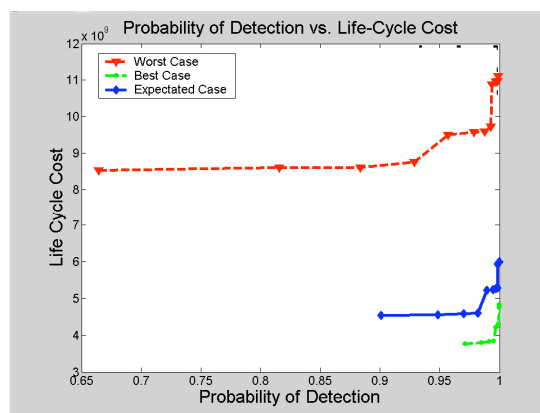


Figure 6: Pareto Front for Three Cases of Uncertainty

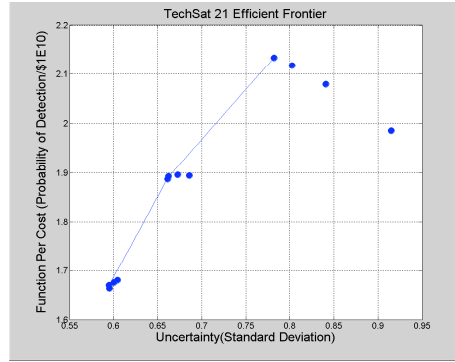


Figure 7: TechSat 21 Portfolio Analysis

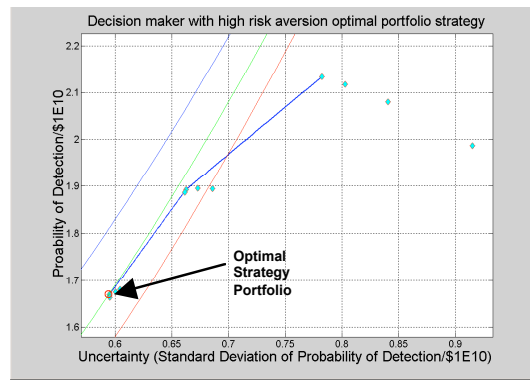


Figure 8: Optimal investment strategy for high risk aversion decision maker

Table 5: Composition of TechSat 21 decision maker strategies

Decision Maker Type	Percentage of Portfolio	Architecture Design Vector {alt,sats/clustr,#clustr,#planes,ant pow,ant_diam}	Total Utility/\$	Uncertainty
High Risk Aversion	100%	{800, 4, 42, 6, 1000, 2.5}	1.67	0.59
Moderate Risk Aversion	100%	{800,4,42,6,900,3}	1.89	0.66
Low Risk Aversion	100%	{800,4,42,6,900,3.5}	2.13	0.78

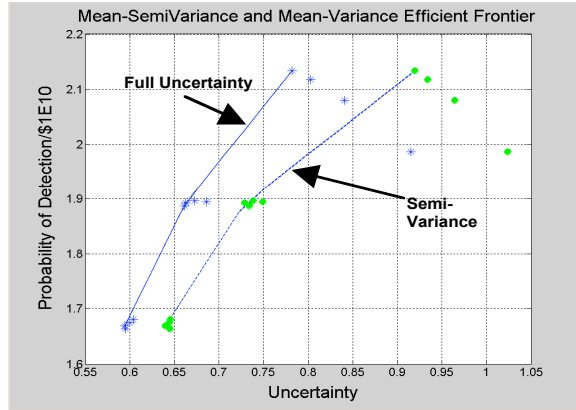


Figure 9: TechSat 21 Portfolio Analysis with full uncertainty and semi-variance

Table 6: Composition of high risk averse optimal portfolio strategy using semi-variance

Decision Maker Type	Percentage of Portfolio	Architecture Design Vector {alt,sats/clustr,#clustr,#planes,ant pow,ant_diam}	Total Utility/\$	Uncertainty
High Risk	100%	{800, 4, 42, 6, 1000, 2.5}	1.67	0.64
Aversion		Complete Portfolio Value and Uncertainty	1.67	0.64
Moderate Risk	100%	{800, 4, 42, 6, 1000, 2.5}	1.67	0.64
Aversion		Complete Portfolio Value and Uncertainty	1.67	0.64
Low Risk	100%	{800,4,42,6,900,3.5}	2.13	0.92
Aversion		Complete Portfolio Value and Uncertainty	2.13	0.92

Table 7: Design vector for the Broadband Communication Satellite System

Name	Description	Potential Values
Altitude	Altitude for a defined circular orbit	LEO(1500km), MEO(20184km), GEO(35786km)
Inclination	The inclination of the circular orbits.	0-90°
Satellites per Plane	The number of satellites in each of the occupied planes	1-8
Number of Planes	The number of orbital planes that the satellite constellation occupies	1-10
Payload Power	Downlink power from an individual satellite	1kW-10kW
Phased Array Area	Area in square meters of the total phased array antenna area	1-5m ²

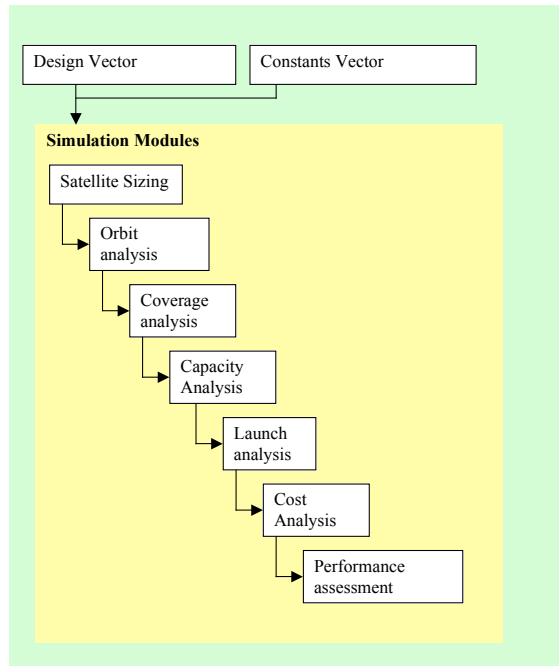


Figure 10: Systems Simulation Flow

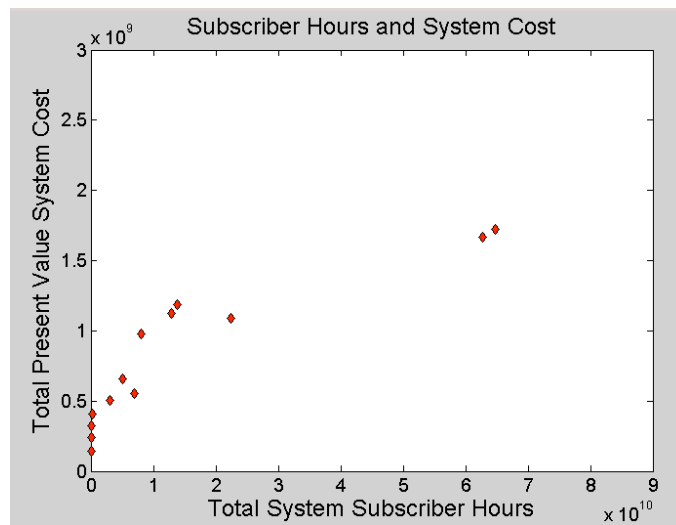


Figure 11: Commercial Broadband System Pareto Optimal Front

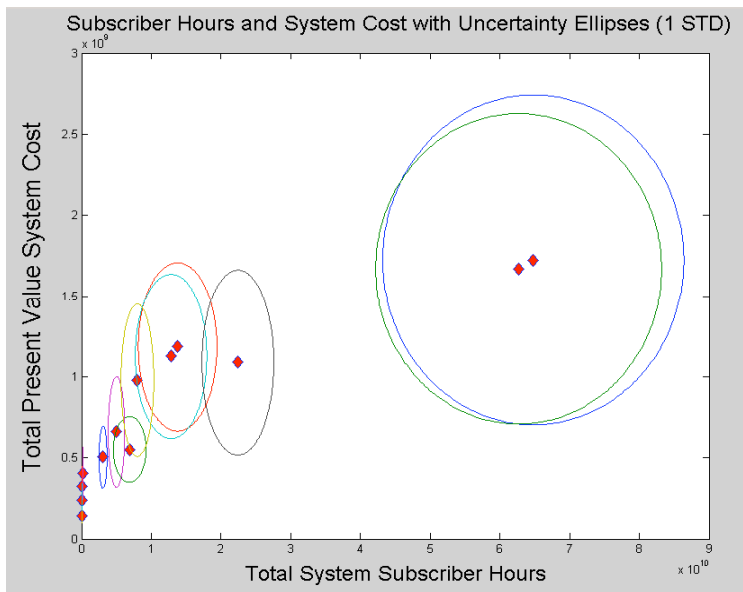


Figure 12: Broadband tradespace with the inclusion of uncertainty

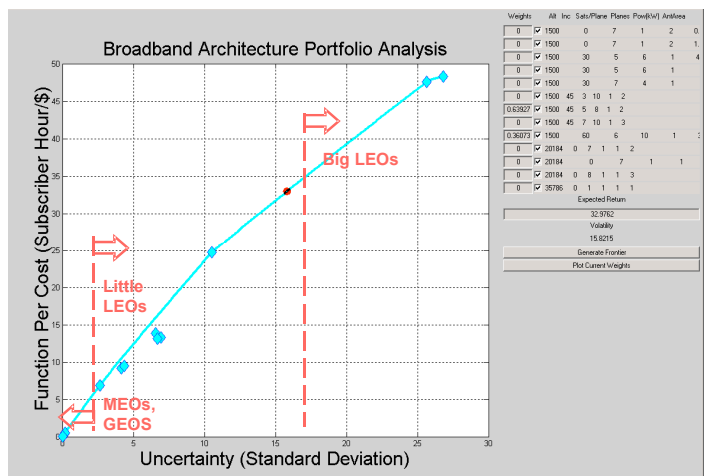


Figure 13: Snapshot of the Architecture Portfolio Flight Simulator

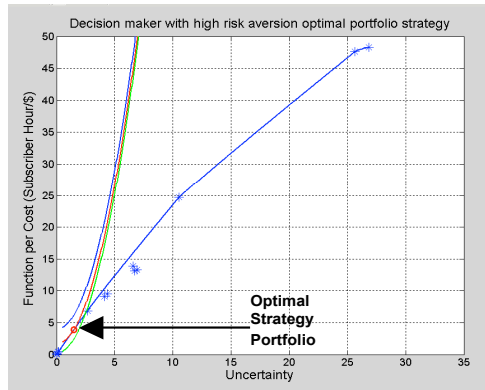


Figure 14: Optimal investment strategy for high risk aversion decision maker

Table 8: Composition of Broadband high risk aversion decision maker strategy

Decision Maker Type	Percentage of Portfolio	Architecture Design Vector {alt, inc, sats/plane, planes, pow, ant area}	Subscriber Hour/\$	Uncertainty
High Risk Aversion	55%	{MEO, 0, 8, 1, 1, 3}	0.5	0.2
	45%	{LEO, 0, 7, 1, 2, 0.5}	6.9	2.7
Moderate Risk Aversion	100%	Portfolio Value and Uncertainty	3.4	1.3
		{LEO, 45, 5, 8, 1, 2}	24.7	10.5
Low Risk Aversion	9%	{LEO, 45, 5, 8, 1, 2}	24.7	10.5
	2%	{LEO, 45, 7, 10, 1, 3}	48.3	26.8
	89%	{LEO, 60, 6, 10, 1, 3.5}	47.6	25.6
		Portfolio Value and Uncertainty	45.5	24.2

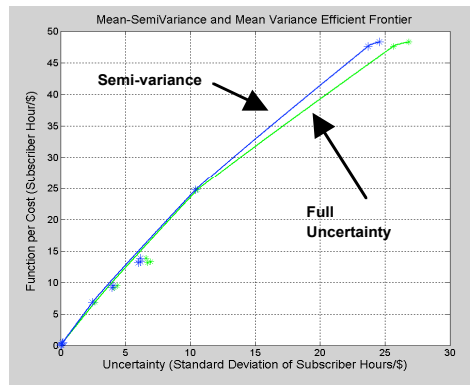


Figure 15: Broadband portfolio analysis with full uncertainty and semi-variance

Table 9: Composition of Broadband high risk aversion decision maker strategy

Decision Maker Type	Percentage of Portfolio	Architecture Design Vector {alt, inc, sats/plane, planes, pow, ant area}	Subscriber Hour/\$	Uncertainty
High Risk Aversion	49%	{MEO, 0, 8, 1, 1, 3}	6.9	1.1
	2%	{LEO, 0, 7, 1, 2, 0.5}	13.3	2.6
	49%	{LEO, 30, 5, 6, 1, 4}	0.5	0.08
Moderate Risk Aversion		Portfolio Value and Uncertainty	3.9	0.63
	100%	{LEO, 45, 5, 8, 1, 2}	24.7	10.5
Low Risk Aversion		Portfolio Value and Uncertainty	24.7	10.5
	24%	{LEO, 45, 7, 10, 1, 3}	48.3	10.4
	76%	{LEO, 60, 6, 10, 1, 3.5}	47.6	9.9
		Portfolio Value and Uncertainty	47.7	9.9

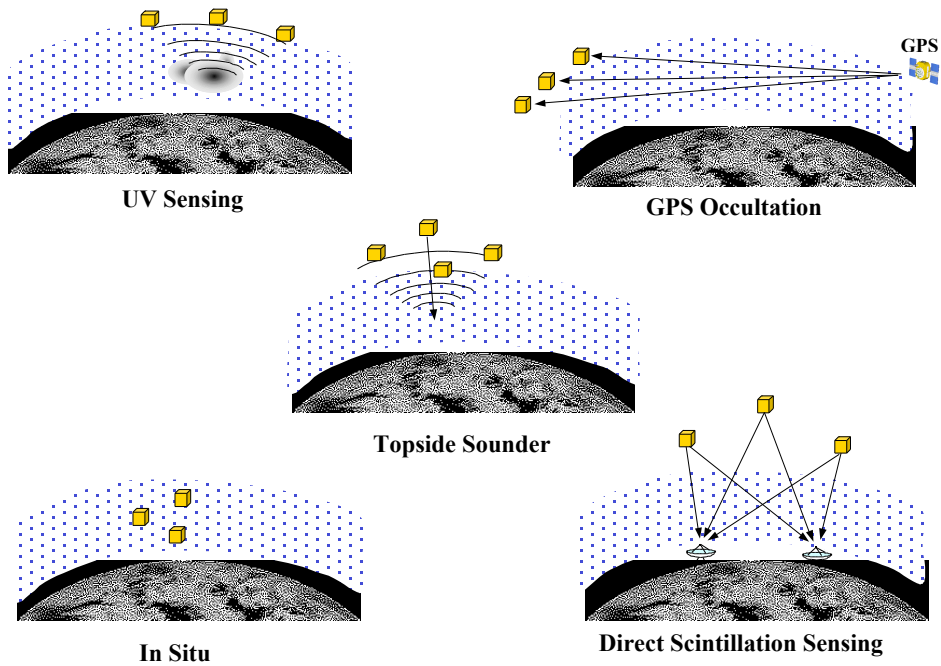


Figure 16: Approaches to Measuring Ionosphere Characteristics

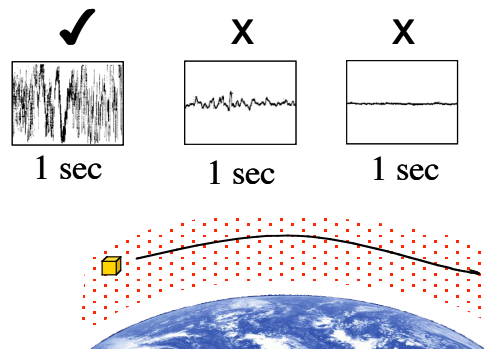


Figure 17: ATOS Low Latitude Survey Mission

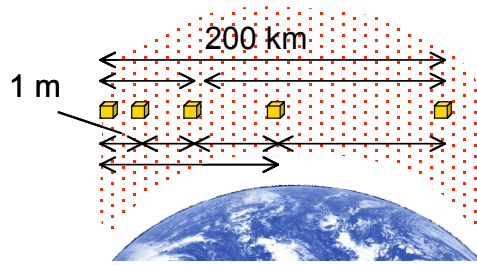


Figure 18: ATOS Low Latitude Snapshot Mission

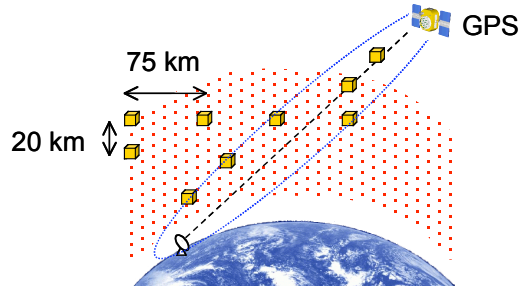


Figure 19: ATOS High Latitude Survey Mission

Table 10: Design vector for the ATOS Satellite System

Name	Description
Altitude	Altitude of the satellite swarm
Subplanes per Swarm	Number of subplanes in swarm
Satellites per Swarm	Number of satellite in swarm
Suborbits per Swarm	The number of concentric orbits in swarm
Subplane Yaw	The yaw angle of the swarm with respect to nadir
Separation Distance	The maximum along track separation

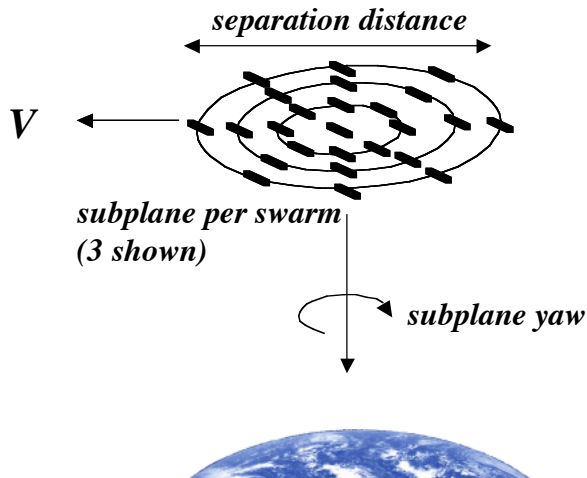


Figure 20: Graphical representation of ATOS Design Vector

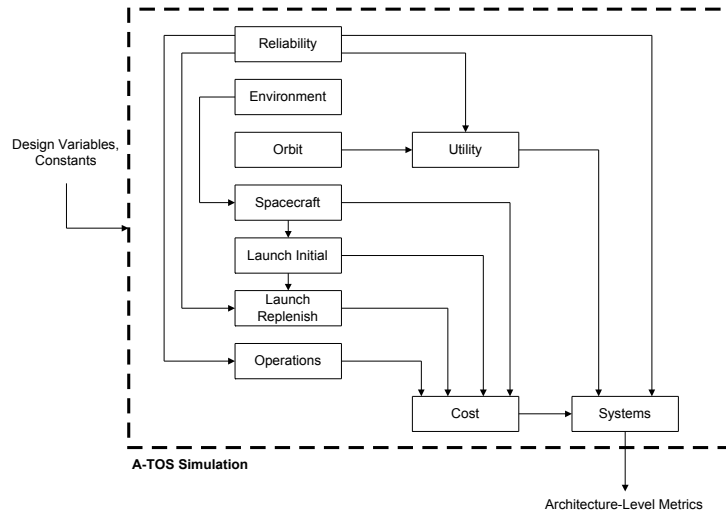


Figure 21: ATOS GINA Model Module Flow Diagram

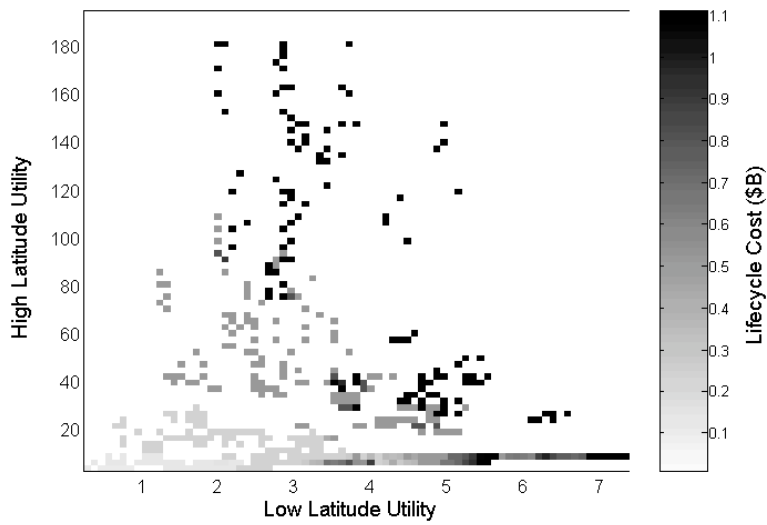


Figure 22: Low and High Utility Tradespace vs. Lifecycle Cost

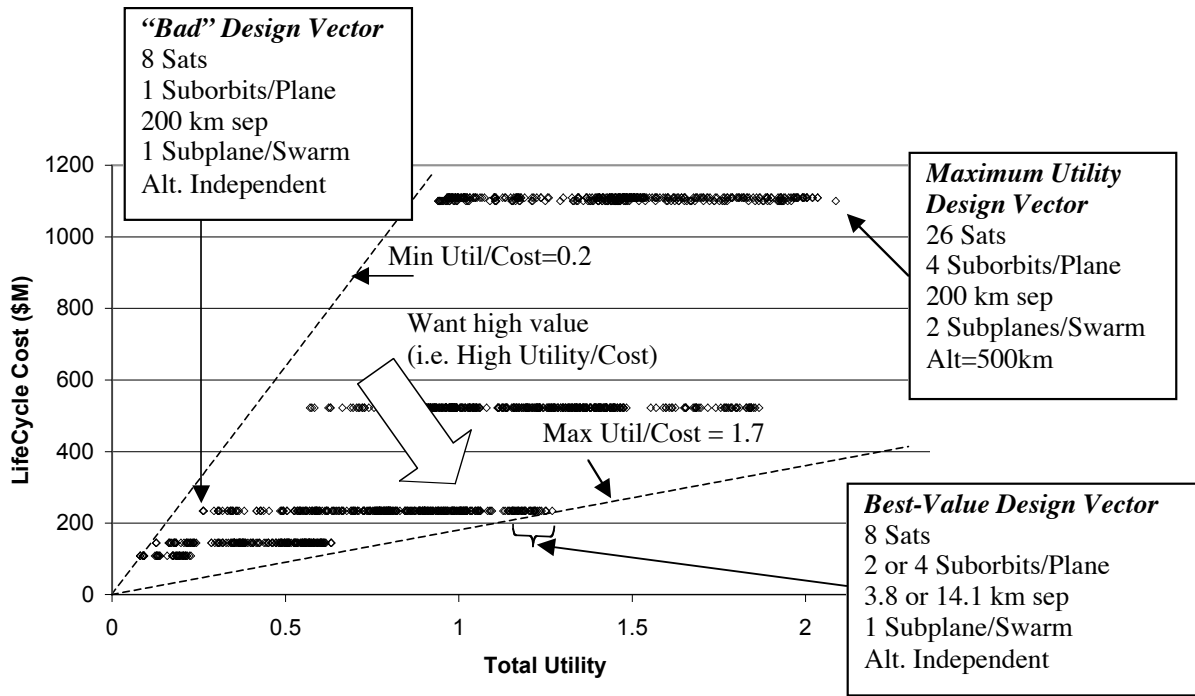


Figure 23: ATOS Cost and Utility Tradespace

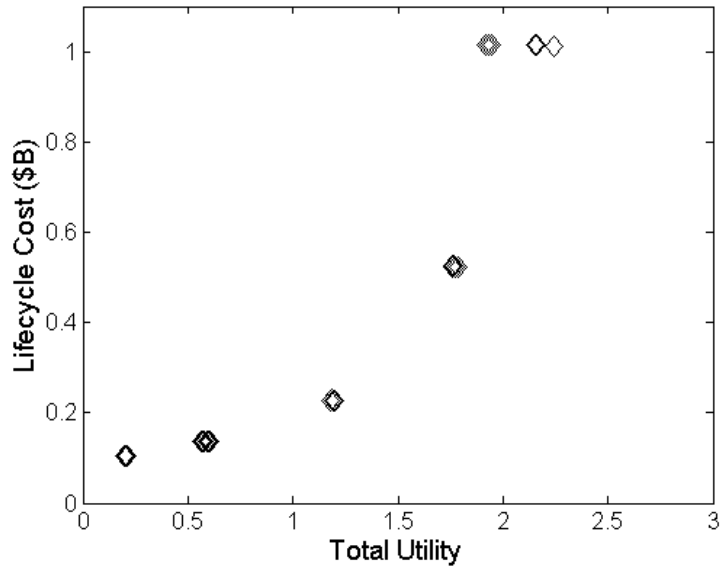


Figure 24: (Near) Pareto Optimal Front for the ATOS Architectural Tradespace

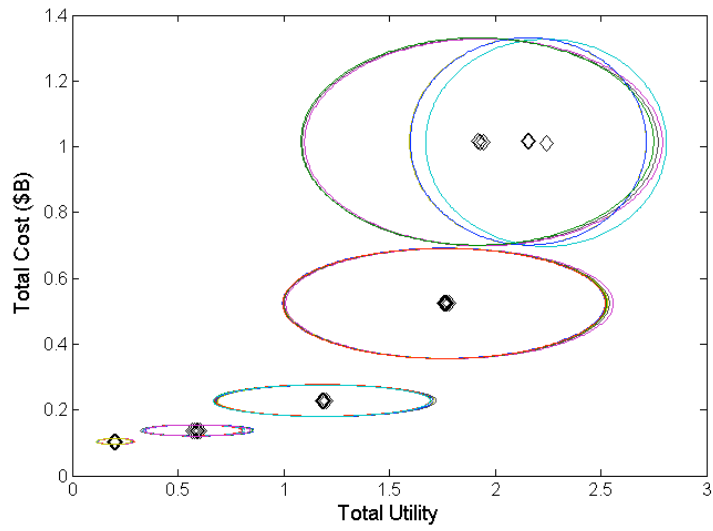


Figure 25: ATOS Utility and Cost Tradespace with Uncertainty Ellipses (1StdDev)

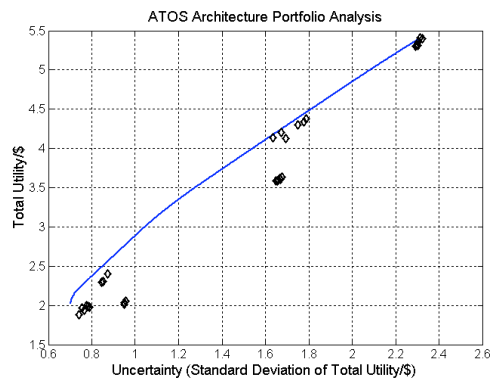


Figure 26: Efficient Frontier in the ATOS tradespace

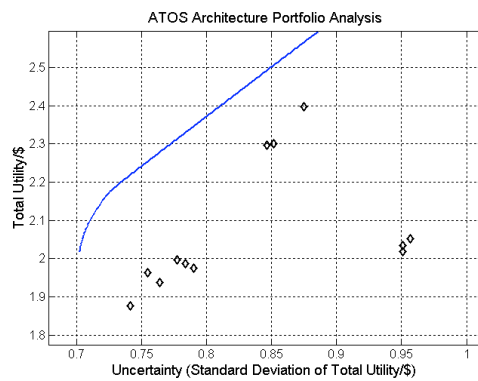


Figure 27: Closer Look at the ATOS Efficient Frontier

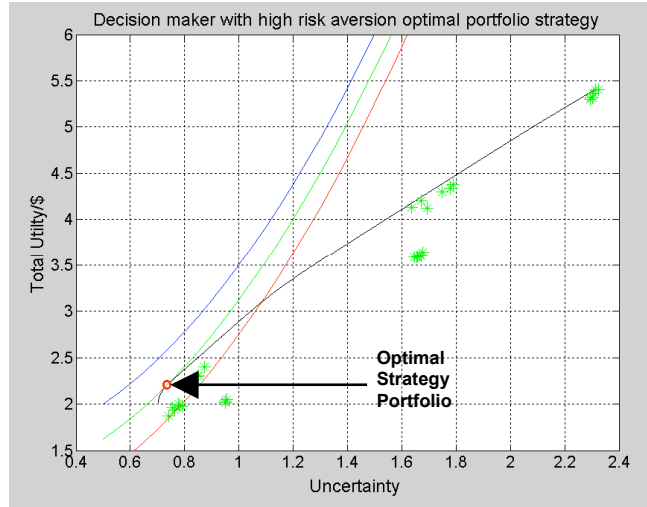


Figure 28: Optimal investment strategy for high risk aversion decision maker

Table 11: Composition of ATOS decision maker strategy

Decision Maker Type	Percentage of Portfolio	Architecture Design Vector {sats/swarm, suborbs,size,yaw,subplanes,alt}	Total Utility/\$	Uncertainty
High risk aversion	52%	{26,4,14.1,60,2,700}	2.4	0.9
	48%	{2,1,3.8,30,1,300}	1.9	0.8
	100%	Portfolio Value and Uncertainty	2.2	0.7
Moderate risk aversion	57%	{26,4,14.1,60,2,700}	2.4	0.9
	28%	{4,2,3.8,30,1,500}	4.2	1.7
	15%	{4,1,14.1,0,1,700}	4.1	1.6
	100%	Portfolio Value and Uncertainty	3.2	1.1
Low risk aversion	83%	{8,4,14.1,30,1,700}	5.4	2.3
	17%	{4,2,3.8,30,1,500}	4.2	1.7
	100%	Portfolio Value and Uncertainty	5.2	2.2

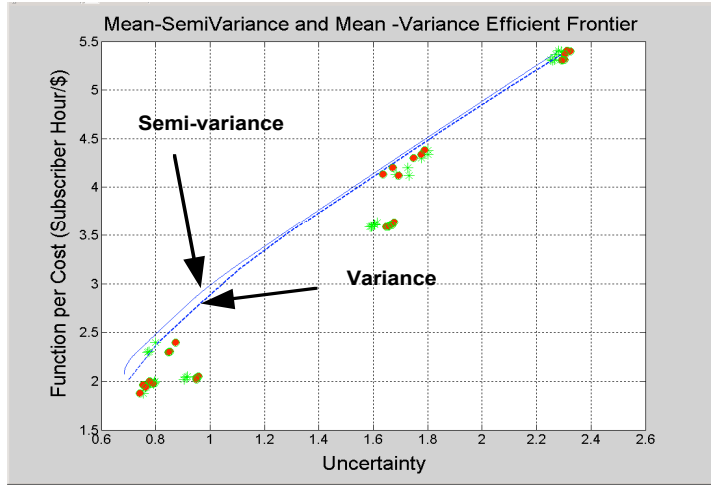


Figure 29: ATOS portfolio analysis with full uncertainty and semi-variance

Table 12: Composition of ATOS high risk aversion decision maker strategy using semi-variance

Decision Maker Type	Percentage of Portfolio	Architecture Design Vector {sats/swarm, suborbs,size,yaw,subplanes,alt}	Total Utility/\$	Uncertainty
High risk aversion	64%	{26,4,14.1,60,2,700}	2.4	0.8
	36%	{2,1,3.8,30,1,300}	2.0	0.8
	100%	Portfolio Value and Uncertainty	2.3	0.7
Moderate risk aversion	65%	{26,4,14.1,60,2,700}	2.4	0.8
	35%	{4,2,3.8,30,1,500}	4.3	1.8
	100%	Portfolio Value and Uncertainty	3.1	1.0
Low Risk Aversion	100%	{8,4,14.1,30,1,700}	5.4	2.3
	100%	Portfolio Value and Uncertainty	5.4	2.3

References

- ¹ Walton, M. (Forthcoming). "Managing uncertainty in the conceptual design of space systems using portfolio theory." Journal of Spacecraft and Rockets.
- ² Shaw, G., D. Miller, and D. Hastings (2001). "Development of the Quantitative Generalized Information Network Analysis (GINA) Methodology for Satellite Systems." *Ibid.* **38**(2): 257-269.
- ³ Jilla, C. (2002). A Multiobjective, Multidisciplinary Design Optimization Methodology for the Conceptual Design of Distributed Satellite Systems. Aeronautics and Astronautics. Cambridge, MA, Massachusetts Institute of Technology. PhD.
- ⁴ Shaw, G. B. (1999). The generalized information network analysis methodology for distributed satellite systems. Aeronautics/Astronautics. Cambridge, MA, Massachusetts Institute of Technology. ScD.
- ⁵ Kashitani, T. (2002). Development and Application of an Analysis Methodology for Satellite Broadband Network Architectures. Proceedings of the 20th AIAA International Communications Satellite Systems Conference, Montreal, Canada.
- ⁶ Larson, W. a. J. W., Ed. (1992). Space Mission Analysis and Design. Torrance, CA, Microcosm.
- ⁷ Kelic, A. (1998). Assessing the Technical and Financial Viability of Broadband Satellite Systems Using a Cost per T1 Minute Metric. Aeronautics and Astronautics. Cambridge, MA, Massachusetts Institute of Technology. SM, SM.
- ⁸ Larson, W. a. J. W., Ed. (1992). Space Mission Analysis and Design. Torrance, CA, Microcosm.
- ⁹ Von Neumann, J. a. O. M. (1944). Theory of Games and Economic Behavior. New York, John Wiley and Sons.
- ¹⁰ Shaw, G., D. Miller, and D. Hastings (2001). "Development of the Quantitative Generalized Information Network Analysis (GINA) Methodology for Satellite Systems." *Journal of Spacecraft and Rockets* **38**(2): 257-269.